

LA-UR--98-1335  
CONF-980412--

## Acousto-Optically Tuned Isotopic CO<sub>2</sub> Lasers for Long-Range Differential Absorption LIDAR

David C. Thompson, George E. Busch, Clifford J. Hewitt,  
Dennis K. Remelius, Tsutomu Shimada, Charlie E.M. Strauss,  
and Carl W. Wilson

Los Alamos National Laboratory, MS E548, Los Alamos, NM 87545

### ABSTRACT

We are developing 2-100 kHz repetition rate CO<sub>2</sub> lasers with millijoule pulse energies, rapid acousto-optic tuning and isotopic gas mixes, for Differential Absorption LIDAR (DIAL) applications. We explain the tuning method, which uses a pair of acousto-optic modulators and is capable of random access to CO<sub>2</sub> laser lines at rates of 100 kHz or more. The laser system is also described, and we report on performance with both normal and isotopic gas mixes.

**Keywords:** LIDAR, DIAL, CO<sub>2</sub>, laser, acousto-optic, tuning, isotopic.

RECEIVED

SEP 22 1998

OSTI

### 1. REQUIREMENTS FOR LONG-RANGE DIAL

Analysis of noise sources in DIAL in the infrared region of the spectrum indicates that the signal-to-noise ratio can be improved if multi-wavelength beams are transmitted at a high repetition rate. The multiple wavelengths and high repetition rate provide uncorrelated data at the fastest rate it can be generated. High-repetition rate can produce more information in a given time: more laser lines, more spatial positions, and more uncorrelated speckles. Rapid line-tuning gives more speckles due to wavelength decorrelation of speckle, more lines for chemical analysis and albedo separation, and more measurements made in times short compared to the time for platform motion or atmospheric changes. Such changes typically take place on a millisecond time scale, so repetition and tuning rates of up to 100 kHz will be useful where ~50- to 100 distinct wavelengths are of interest, as in the case of CO<sub>2</sub> lasers.

Moreover, shorter pulses can improve signal-to-noise ratio (SNR). The short pulse with its narrow (in time) sampling window more effectively uses the available pulse energy and reduces the noise-equivalent-energy due to thermal background noise and other white noise sources by the square root of the pulse length.

For long range DIAL, atmospheric concentrations of CO<sub>2</sub> give rise to significant absorption loss (up to 20 %/km depending on atmospheric conditions). By using isotopic CO<sub>2</sub> lasers this loss can be made negligible. We have used lasers with <sup>13</sup>C<sup>16</sup>O<sub>2</sub> and <sup>13</sup>C<sup>18</sup>O<sub>2</sub> isotopes, as well as the normal <sup>12</sup>C<sup>16</sup>O<sub>2</sub>.

Table 1 shows our immediate and long-term goals for transmitter performance.

### 2. ACOUSTO-OPTIC TUNING

Acousto-optic tuning provides simple and flexible electronic control of laser cavity wavelength, as well as of other cavity parameters such as cavity length, loss and out-coupling fraction.

DISTRIBUTION OF THIS DOCUMENT IS UNLIMITED

MASTER

### **DISCLAIMER**

This report was prepared as an account of work sponsored by an agency of the United States Government. Neither the United States Government nor any agency thereof, nor any of their employees, makes any warranty, express or implied, or assumes any legal liability or responsibility for the accuracy, completeness, or usefulness of any information, apparatus, product, or process disclosed, or represents that its use would not infringe privately owned rights. Reference herein to any specific commercial product, process, or service by trade name, trademark, manufacturer, or otherwise does not necessarily constitute or imply its endorsement, recommendation, or favoring by the United States Government or any agency thereof. The views and opinions of authors expressed herein do not necessarily state or reflect those of the United States Government or any agency thereof.

## **DISCLAIMER**

**Portions of this document may be illegible in electronic image products. Images are produced from the best available original document.**

## Desired laser performance

Parameter	Now	Long-term
Pulse repetition rate	5 kHz	100 kHz
Tuning rate	5 kHz	100 kHz
Pulse energy	2 mJ	5 mJ
Pulse length	100-300 ns	1-20 ns
Average Power	10 W	500 W
Beam Quality ( $M^2$ )	1.5	1.2
Gas-fill Lifetime	$> 10^4$ hr	$> 10^4$ hr

Table 1. Immediate and long-term DIAL transmitter system goals.

To date, rapidly tuned lasers have most often used small galvo-driven mirrors or gratings to randomly access wavelengths at rates up to about 200 Hz,<sup>1-3</sup> or have used rapidly rotating mirrors or prisms to sequentially tune through wavelengths at speeds up to 40kHz in bursts at a few hundred Hz.<sup>4,5</sup> However speeds remain limited by inertia, mechanisms are bulky and hard to align, and higher speeds and random access are difficult.

Acousto-optic (AO) devices have provided means to replace slow moving parts with faster devices, which are electronically controlled and have no moving parts. Reference 6 gives a useful review of a variety of AO devices, including modulators (AOM's), deflectors (AOD's) and AO tunable filters (AOTF's). An AO device is shown schematically in Figure 1.

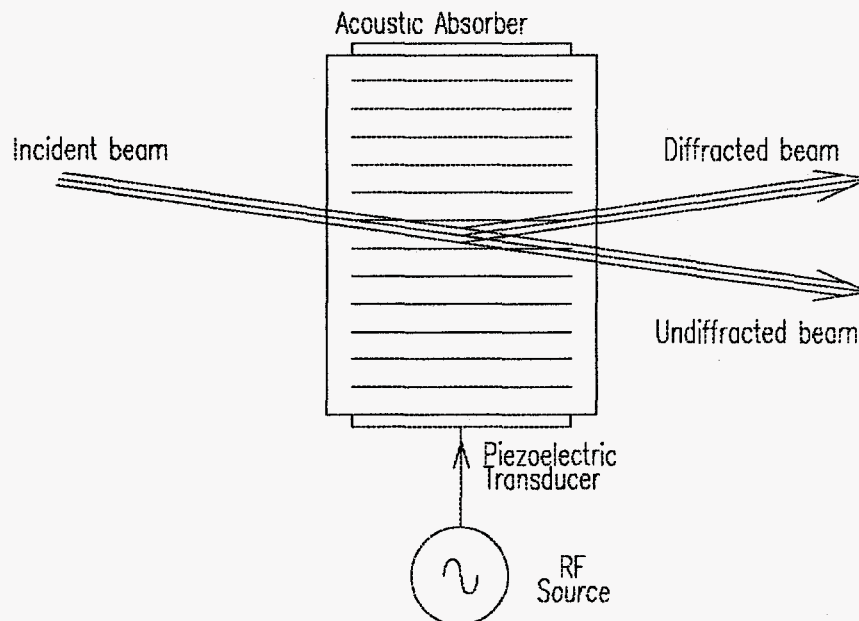


Figure 1. An AO device. The RF source drives the piezoelectric transducer, producing an acoustic wave. Peak efficiency results when both incident and diffracted beams are at the Bragg angle,  $\theta_B$ , to the acoustic wave-fronts.

Momentum conservation between the sound and light waves requires that the incident and diffracted light waves (of free-space wavelength  $\lambda_0$ ) each be at an angle  $\theta_B$  with respect to the sound wave-fronts (with frequency  $\nu$  and velocity  $V_a$ ), for efficient diffraction.  $\theta_B$ , the Bragg angle (within the medium with refractive index  $n_0$ ), is given by

$$\sin \theta_B = \frac{\lambda_0 \nu}{2n_0 V_a} \quad (1)$$

When the interaction length between light and sound is long enough (the Bragg regime), the theory of AO interactions<sup>7,8</sup> predicts that the incident wave is diffracted into one (first order) diffracted wave with an efficiency that depends on the acoustic power and with essentially 100% efficiency at the correct acoustic power. While a number of effects can reduce this efficiency, these can usually be made quite small. In Figure 2, we show the efficiency achieved for the device we have used (Isomet model 1208-6). We see that a diffraction efficiency of over 97% is obtained. Combined with static loss due to losses at AR-coated surfaces and absorption in the Ge, we obtain an overall single-pass efficiency of about 95% at shorter wavelengths, decreasing to 92 or 93% at longer wavelengths, due to increased static loss.

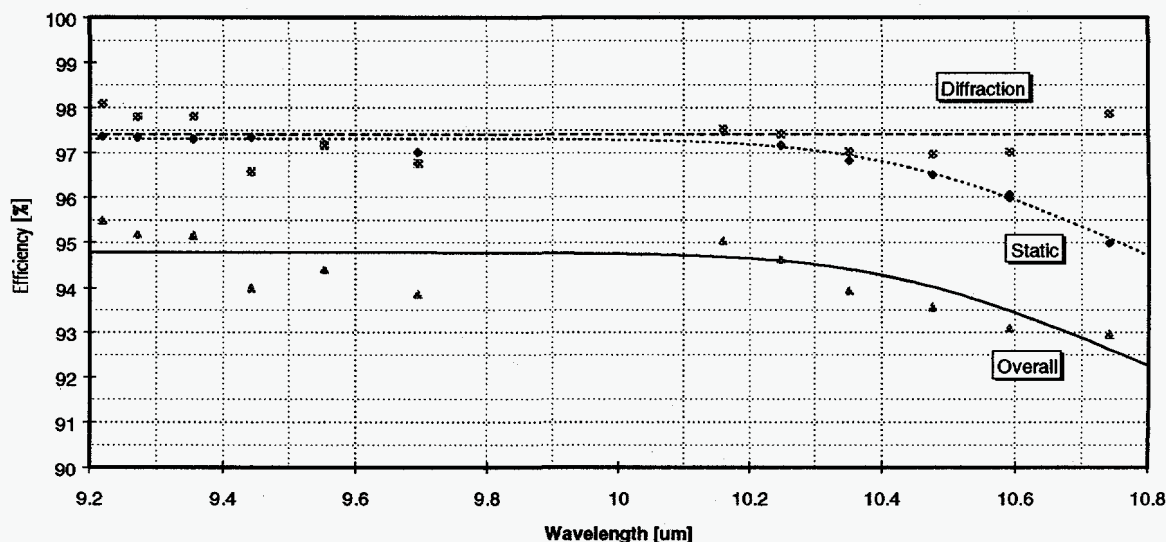


Figure 2. Static and diffraction efficiency of AOM used for tuning (Isomet model 1208-6).

AO tuning has typically involved either combinations of AO deflectors and reflection gratings<sup>9-11</sup> or AOTF's.<sup>12,13</sup> We tune the laser using the configuration shown in Figure 3. A pair of AO modulators each deflect the light. A plane mirror forms one end of the cavity and the incident and diffracted beams are each at the Bragg angle  $\theta_B$  for both AO devices. With the constant deflection angle  $2\theta_B$  for each device determined by the cavity geometry, the wavelength  $\lambda$  is directly determined through Equation 1 by the acoustic frequency  $\nu$  for a given acoustic velocity  $V_a$ . Since bandwidths of the order of an octave or more are routinely achieved for AO devices, very wide tuning ranges are possible, limited in most cases by the spectral width of the gain medium. In our case, for a spectral range of 9.2-11.2  $\mu\text{m}$ , a 20% bandwidth is needed. The discrimination against other nearby wavelengths is determined, as for a grating, by the number of grating "lines" illuminated. In this case, this is the number of acoustic wavelengths illuminated by the beam, multiplied by four due to the two passes through the two AO devices.

There must be two AO modulators because not only is the diffracted beam deflected, but it is also shifted in frequency by the acoustic frequency  $\nu$ , with the direction of the shift depending on the relative orientation of the optical and acoustic beams. This frequency shift accumulates as the light makes multiple passes of the cavity and prevents single-frequency operation.<sup>14</sup> In the case of narrow lines, as in low-pressure  $\text{CO}_2$ , if there is low gain or the need for many round trips inside a laser

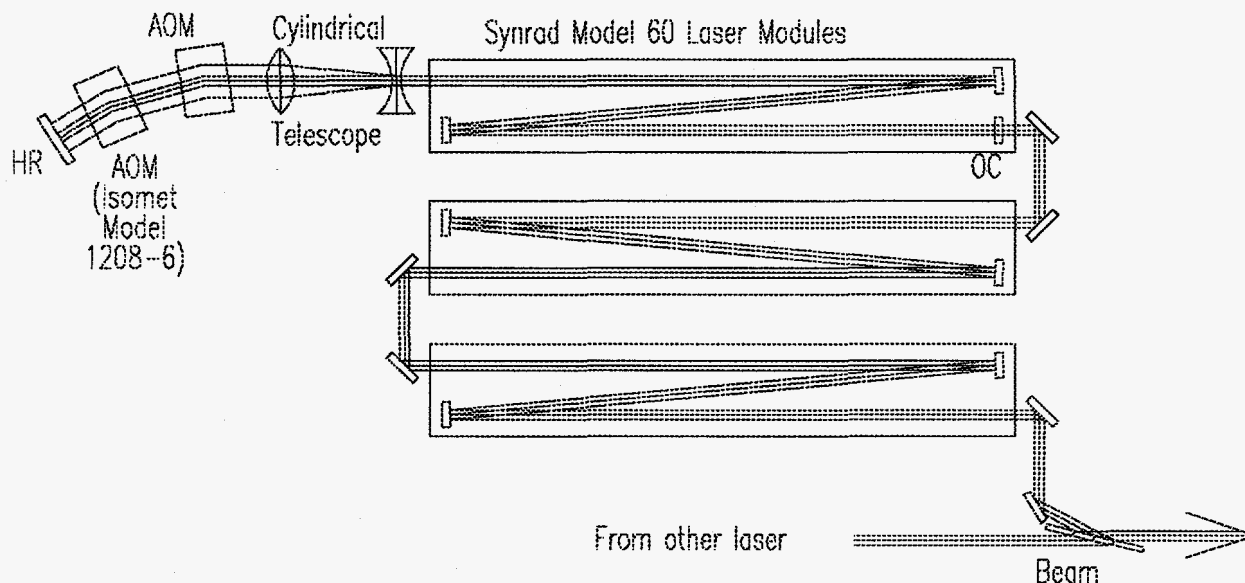


Figure 3. Schematic of AO-tuned laser, including oscillator and amplifiers.

cavity, the frequency shift prevents lasing altogether. The paired modulators, oriented in opposite directions cancel this frequency shift as well as doubling the resolution of the tuner.

The CO<sub>2</sub> gain module is a Synrad Model 60 laser module, with the usual high reflector replaced with a window. The Z-folded 6mm-square waveguide with an overall length of 3.2m gives a beam diameter (to  $1/e^2$  intensity points) of approximately 4 mm. Since this diameter is insufficient to give adequate resolution, a 2.5X afocal cylindrical telescope consisting of ZnSe cylindrical lenses of -2" and +5" focal lengths is used to expand the beam to a diameter of 10mm before passing through the two modulators. The resulting resolution of about 580 is sufficient to give lasing on single lines only, even for the closely-spaced ( $\sim 1 \text{ cm}^{-1}$ ) lines of the 9R branch of CO<sub>2</sub>.

Since the selected wavelength is always at the Bragg angle, the diffraction efficiency of the devices is maximized. This is particularly important in this configuration since the beam is diffracted four times during each cavity round trip.

One important advantage of this latter method of tuning is the ready availability and technical maturity of the components required. The control systems use well-developed RF technology and avoid the use of the high voltages needed for electro-optic components. Since the diffraction angle is fixed, AO modulators are used rather than more complex deflectors. AO modulators are simple, rugged and available in many materials and for many frequency and wavelength ranges. For this application, we use standard commercial Germanium IR modulators.

Since modulation of the acoustic power in the AO modulators is straightforward, the same AO devices are used to Q-switch the laser as well as tune it. Since the cavity feedback is via the first order in both devices, this Q-switch has essentially zero transmission when off. This is a very important attribute for high-gain lasers. The speed of Q-switching is determined by the acoustic transit time. For the 10mm expanded beam and an acoustic velocity of  $5.5 \text{ mm}/\mu\text{s}$  in Ge, this is about  $2 \mu\text{s}$ , but switching is observed to take a small fraction of this, less than 200ns. This is attributed to increased diffraction losses in the cavity as the transverse mode of the laser is disrupted by the acoustic wavefront crossing the beam. This would increase the speed with which the mode is turned on or off. Faster switching without loss of spectral resolution could be obtained if the beam size through one AOM were made smaller and the beam through the other made larger, through the use of a telescope between the two modulators.

In our system, the RF frequency for tuning is generated by a digitally-controlled synthesizer (NEOS model N64010-200-2ASDFS) which can change frequencies in  $< 1 \mu\text{s}$ . The output of the synthesizer is split and each signal is amplified by a

voltage-controlled amplifier (VCA) (Isomet model IA-100) and a power amplifier (Kalmus model 172F) to provide the necessary RF power of ~85W, tunable from 70-90 MHz, required by each AOM. The control inputs to the VCA's are driven by digital-to-analog converters with digital inputs from the computer control system. Since the RF power required to reach maximum diffraction efficiency varies in proportion to the square of the wavelength, variation of the RF power as the wavelength is tuned is necessary if the highest efficiencies are to be achieved.

Tuning rates of up to 70 kHz, with lasing on up to 54 lines, have been achieved by this method. The rate limitation is not the speed of the acousto-optic devices, which would have an upper limit of about 500 kHz due to the transit time, but rather the gain recovery time of the laser. At higher repetition rates the laser becomes unstable, with gain coupling between different lines resulting in a stronger line "robbing" all the gain from weaker lines. We expect this can be remedied by using a laser with faster response, such as a waveguide laser with a smaller waveguide and higher gas pressure.

Since intracavity powers can be several Watts, there is measurable thermal lensing in the AO modulators. Germanium has relatively high acousto-optic efficiency for given acoustic power, good mechanical properties and high thermal conductivity. However, its high value of  $dn/dT$  and relatively high optical absorption coefficient are drawbacks. As a result of thermal lensing, the optimum laser settings for each line depend on the average absorbed optical power and thus on the sequence of lines the laser is operating on, rather than just on the individual line. The overall effect of thermal lensing can be partially compensated by a defocus of the cylindrical telescope, but ultimately the average intracavity laser power is limited by this effect.

### 3. TRANSMITTER CONFIGURATION AND RESULTS

A block diagram of the complete LIDAR transmitter is shown in Figure 4. The normal ( $^{12}\text{C}^{16}\text{O}_2$ ) laser consists of an AO-tuned oscillator with one gain module and two modules as amplifiers, while the isotopic ( $^{13}\text{C}^{18}\text{O}_2$ ) laser uses two modules for the AO-tuned oscillator and a single amplifier. The outputs of the two lasers, with orthogonal polarizations, are combined with a thin-film polarizer. They are then spatially filtered to remove much of the high-order spatial mode content, at the expense of about a 20% loss of power. A pair of AR-coated ZnSe wedges split off small portions of the beam for various diagnostics, described later, prior to expansion of the beam in an off-axis telescope to form the final transmitted beam.

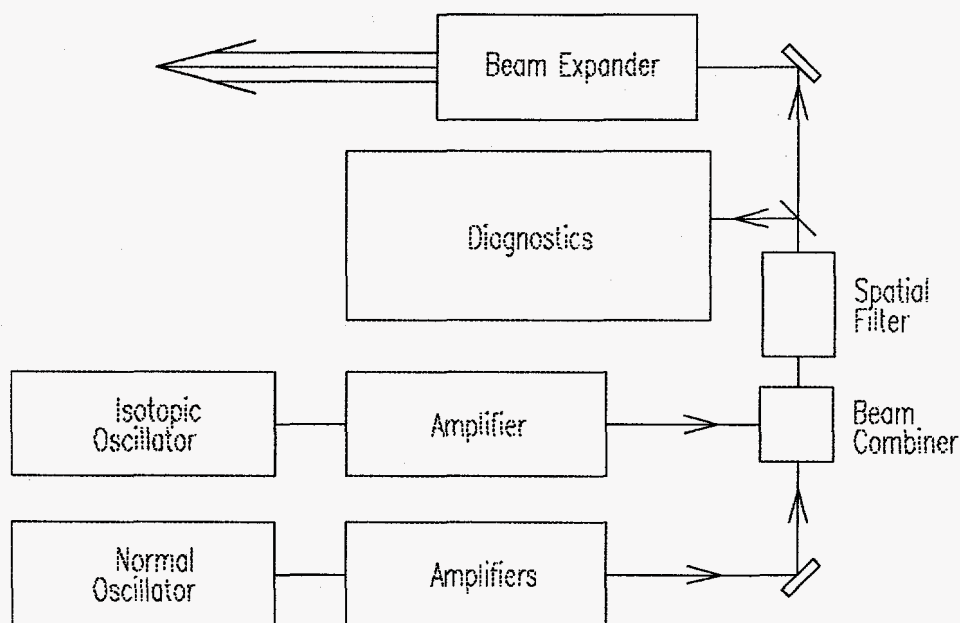


Figure 4. Block diagram of transmitter, showing normal and isotopic oscillators and amplifiers, beam combiner, spatial filter, diagnostics, and beam expander.

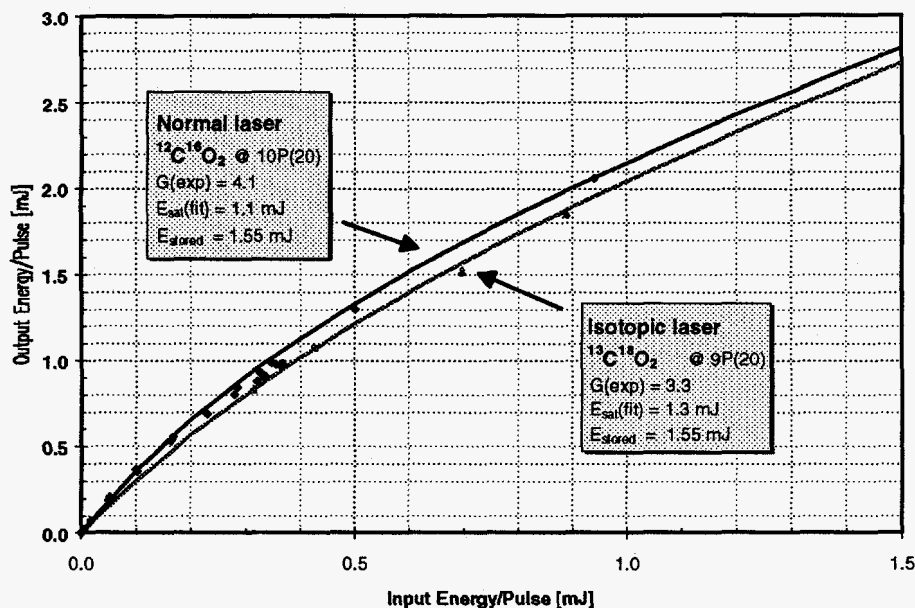


Figure 5. Comparison of saturation and stored energy for normal ( $^{12}\text{C}^{16}\text{O}_2$ ) and isotopic ( $^{13}\text{C}^{18}\text{O}_2$ ) lasers.

Two gain modules are used for the isotopic oscillator since the gain is about 15% lower than for the normal isotope, and the round-trip gain in the oscillator results in better performance over a greater number of lines. It is interesting to note that the lower gain coefficient in the isotope is compensated by a larger saturation energy, resulting in very similar stored energies in the two isotopes. This can be seen in Figure 5, where the gain characteristics for a single gain module are very similar. Moreover, the gains for the long and short wavelength bands are fairly similar. This is not the case for  $^{13}\text{C}^{16}\text{O}_2$ , where the short wavelength bands have much (~60%) lower gain coefficients, resulting in significant difficulty in obtaining reliable operation over the entire wavelength range with a single oscillator configuration. This leads us to conclude that  $^{13}\text{C}^{18}\text{O}_2$  is a good choice than  $^{13}\text{C}^{16}\text{O}_2$  for an isotopic  $\text{CO}_2$  laser.

We have found that good sealed-off laser lifetime can be obtained after passivation consisting of several cycles of refilling and RF discharge pumping. After 5 passivation cycles the  $e^{-1}$  exponential decay time for CW laser power increases to over 9000 hours, or a time to 80% power of greater than 2000 hours of operation.

The combination of the two lasers gives good spectral coverage from 9.2 to 11.1  $\mu\text{m}$  with few gaps. This can be seen in Figure 6, which shows the output pulse energies (prior to combining and spatial filtering) from the two lasers. The percentage fluctuation in the powers are also shown. The lasers were operating at 5 kHz repetition rate. The normal isotope laser energies were measured while operating on each line singly, while the energies for the isotopic laser were measured while scanning over all 49 lines. Those latter energies were then calculated from the areas under the pulse waveforms from a fast Mercury-Cadmium-Telluride (MCT) detector, which had been cross-calibrated to a calorimeter. We also see from the figure that the energy stability is quite good and that the stability during rapid tuning is comparable to stability in single line operation.



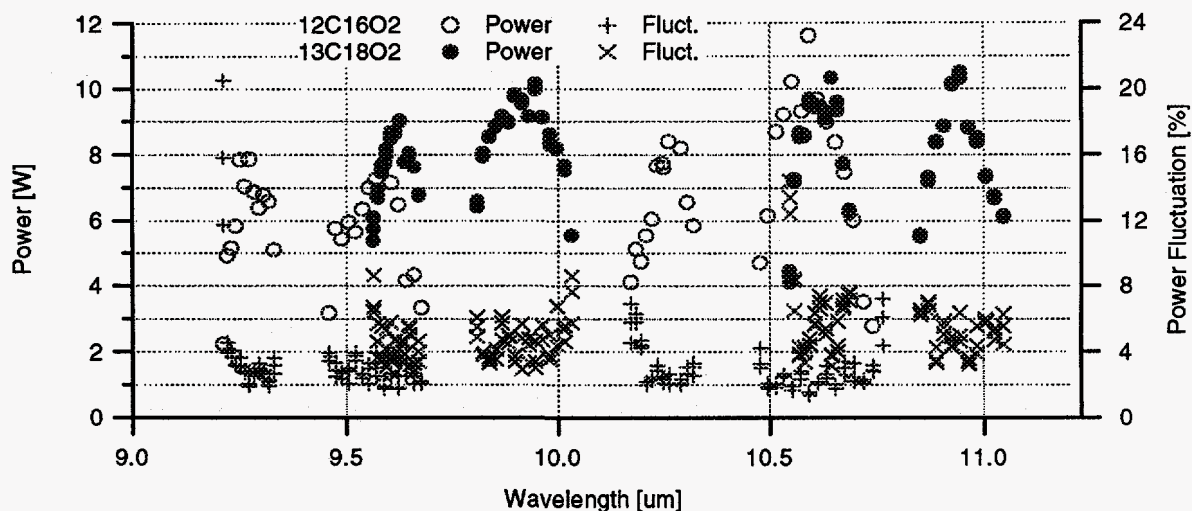


Figure 6. Pulse energy and fluctuation in energy for 52 lines of  $^{12}\text{C}^{16}\text{O}_2$  laser and 49 lines of  $^{13}\text{C}^{18}\text{O}_2$  laser.  $^{12}\text{C}^{16}\text{O}_2$  results are for single-line operation, while  $^{13}\text{C}^{18}\text{O}_2$  results are while scanning over all 49 lines.

Typical pulse shapes for the normal isotope are shown in Figure 7, with pulse widths (FWHM) of about 150ns for a strong line and about 250 ns for a weaker line. Figure 8 shows the variation over all lines, with widths for most lines between 150 and 200 ns and a width of about 350ns for the weakest line. The fluctuation in pulse width is also shown and ranges from less than 1% to about 4%. As expected, the delay from Q-switch turn-on to the laser pulse leading edge varies also, from about 4.1 to 5.0  $\mu\text{s}$ . Though not evident in the waveforms of Figure 7, the end of the Q-switch pulse, corresponding to turning off the RF to the AOM's, is timed to coincide with the trailing edge of the laser pulse so as to remove any long tail. Pulse widths from the isotopic laser are somewhat longer, ranging from 200 to 300 ns for most lines and up to 700 ns for the weakest line. Longer pulse lengths are to be expected for the isotopic laser because pulse length scales with cavity length, which is greater for the isotopic laser because two laser modules are used in the oscillator. The delays range from 4 to 6  $\mu\text{s}$ . They, and the associated jitter, are plotted in Figure 9.

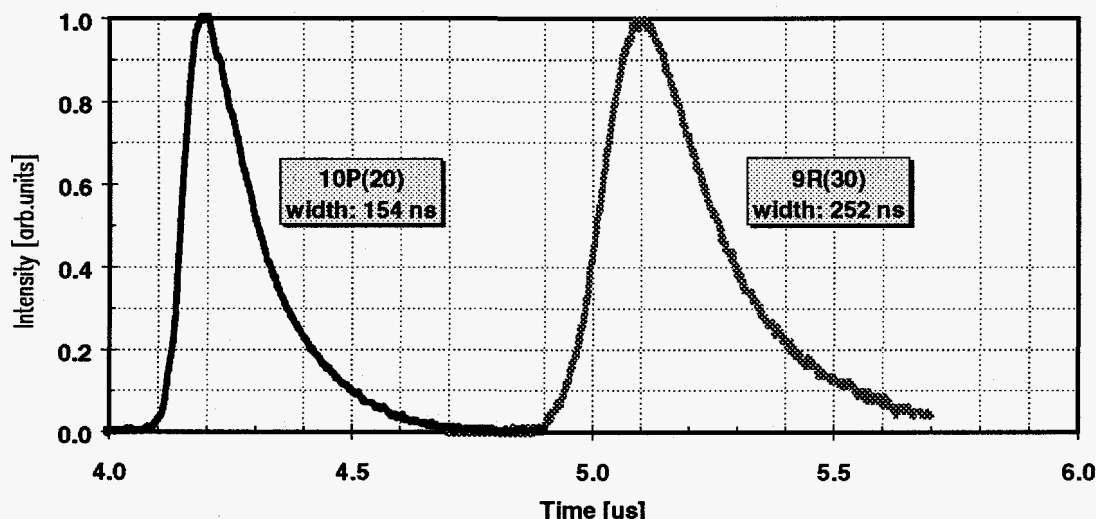


Figure 7. Pulse shapes for 2 lines of the normal isotope laser, normalized to peak power.

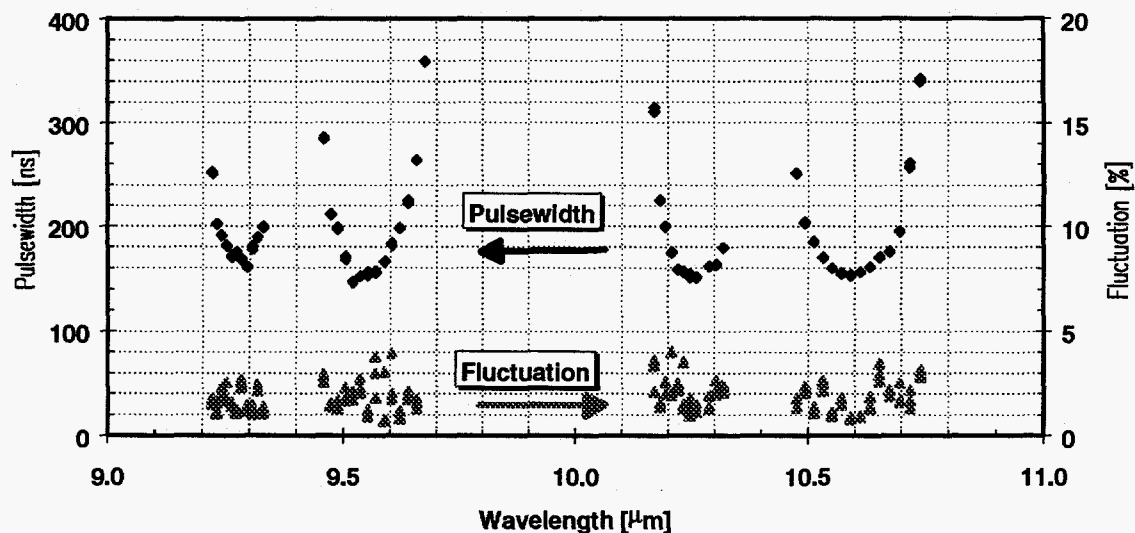


Figure 8. Pulse length and stability for normal isotope laser.

Figure 10 shows the dependence on wavelength of the divergence of the output of the final amplifier for the normal isotope. The divergence is larger in the vertical direction than in the horizontal, even though the waveguide has a square cross-section. This could be due to the asymmetry in the AO tuning optical system, though the effect could be expected to be reduced after passage through the two amplifiers. Alternatively, this may be due to asymmetries in the gain within the waveguides. Though the divergences are different, both fit quite well to the wavelength dependence expected for a beam waist of fixed size at the waveguide exit, as could be expected for a waveguide mode. Also shown in the figure are the variations in pointing with wavelength which show deviations from the mean of less than 5% of the divergence for all but a few of the weakest lines, which range up to 9%.

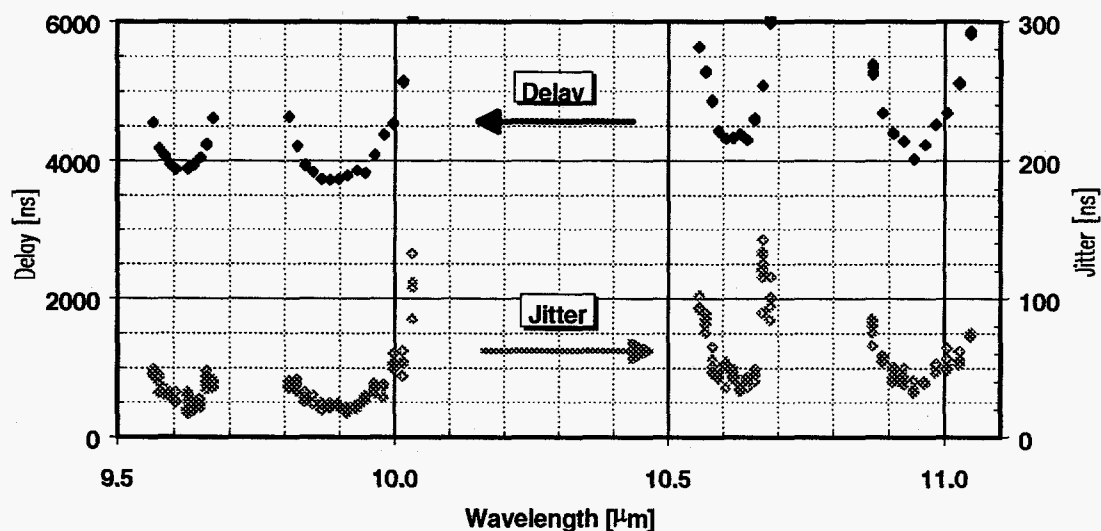


Figure 9. Pulse delay and jitter for isotopic laser.

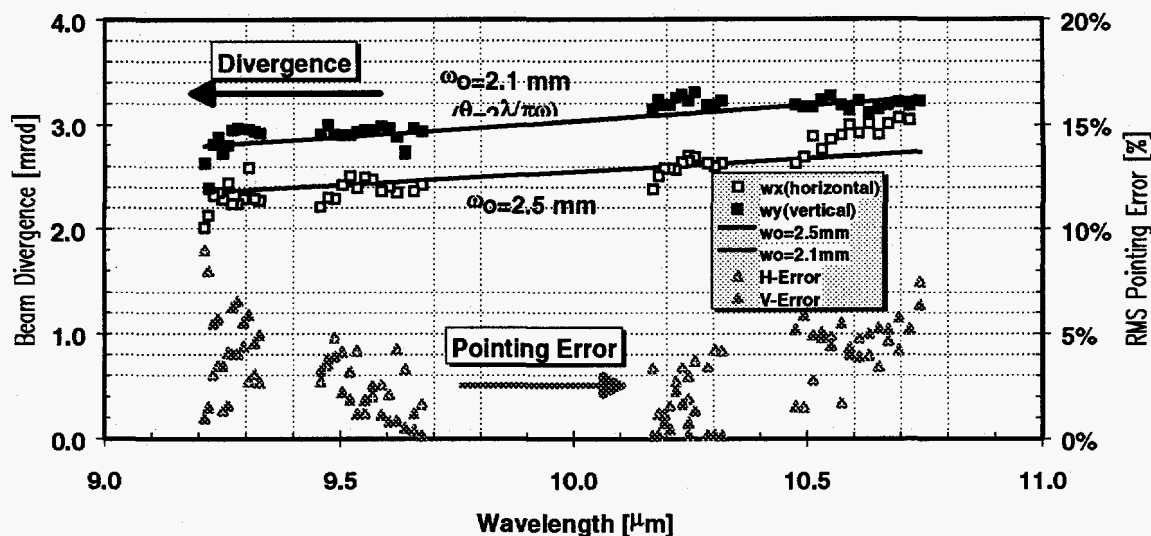


Figure 10. Wavelength dependence of divergence and pointing, for normal isotope laser.

In order to investigate scaling the system to higher average powers, we have configured the isotopic system with the usual two-module oscillator and increased the number of amplifier modules to three. With this system we increased repetition rate from 5kHz to 10kHz, the limit of the present control system, while scanning over 44 lines. The results are shown in Figure 11, with the oscillator output plotted at several repetition rate values from 5 to 10kHz and the outputs from each successive amplifier plotted for 5 and 10kHz only. The results are not fully optimized at the higher repetition rates, since neither the duty cycle of the RF pump to the laser modules, nor the parameters for AO tuning were varied from their 5kHz values. We see that it is possible to get from 30-50% more power at 10kHz, but that the pulse energy is decreasing by 25-35%. We also see the decreasing effect of adding additional amplifiers.

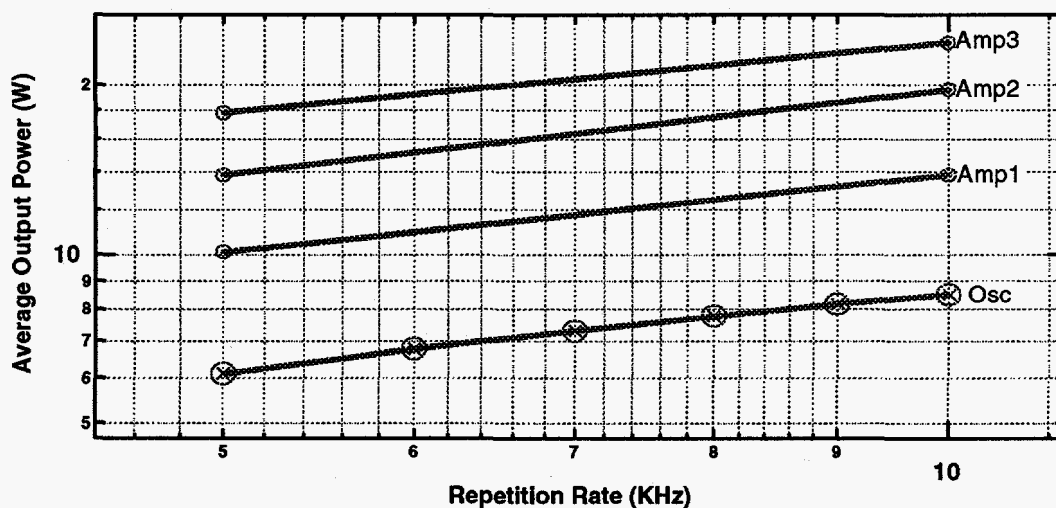


Figure 11. Scaling of isotopic laser results with additional amplifiers and to 10kHz. The laser is scanning over 44 lines. The oscillator output was measured every kHz from 5 to 10kHz, while the amplifier outputs were only measured at 5kHz and 10kHz.

#### 4. DATA ACQUISITION AND CONTROL SYSTEM

Tuning the laser system over more than 50 lines, at high rates, puts significant demands on a control system. For optimum performance, values for parameters such as Q-switch timing must be changed for each line. We have developed fast computer control systems to meet these needs.

The requirements for data acquisition and control systems are as follows. One or two lasers must be controlled simultaneously. The system must independently control the timing of RF excitation for up to 6 laser modules and must control RF frequency and amplitude and Q-switch timing for 2 AO tuners. In general all parameters vary for each line, at 5-10kHz or more, with up to 50 or more distinct lines for each laser. The system must also control and collect data from box-car integrators, transient digitizers, etc. and provide for storage and real-time display and analysis of LIDAR return and diagnostic data.

We have used two types of systems to meet these requirements. In the laser laboratory, we control a single AO-tuned laser using a system based on a personal computer with a National Instruments analog-to-digital converter card for data acquisition and a VXI crate interfaced to the PC with a PCI/MXI interface containing a fast digital sequence generator (Berkeley Nucleonics model DG600). The latter has 48 output bits clocked at 50MHz and is used to control the digital frequency synthesizer for tuning, a pair of 8-bit digital-to-analog converters that control the two AO tuner VCA's, and several triggers. The system is programmed with Labview software running under the Windows operating system. This system uses relatively inexpensive commercial components and is very flexible. However it has relatively limited capabilities for real-time adjustment of parameters and for real-time display and analysis of data.

For our field system, we use a data acquisition and control system based on UNIX workstations and a number of VME components, including an embedded real-time controller and several custom cards. The latter include a field-programmable gate array (FPGA) - based controller that provides most of the timing and control functions for AO tuning of two lasers at rates up to 10kHz, including real-time adjustment of laser parameters. The system also provides many advanced capabilities for data storage and real-time operator interaction and analysis

#### 5. DIAGNOSTICS

Diagnostics for the transmitter include a reference detector for DIAL, power meters, a far-field spatial diagnostic and a spectrometer. Four diagnostic beams are generated by reflections from AR-coated surfaces (with about 1% broadband reflectivity) of two ZnSe wedges in the combined and spatially filtered laser output beam. The reference detector consists of a 1mm square TE-cooled photo-conductive MCT detector (VIGO System model PC-L-2TE) at the focus of a 2" focal-length lens. A calibrated power meter is operated full-time on one of the four diagnostic beams. The far-field spatial diagnostic consists of a 120 X 120 element pyroelectric array (Spiricon Pyrocam II) at the focus of a mirror to give the far-field profile of the outgoing laser beam.

Rapid tuning requires new diagnostics to examine performance on single lines while the laser is being rapidly tuned through many lines, since laser performance is not necessarily the same as when operating on a single line. This capability was provided for the Pyrocam, whose response is limited to about 100Hz, and a linear pyroelectric array at the focal plane of the spectrometer (Spiricon model LP-128-22). Initially, a fast mechanical chopper was used, operated so that while the laser sequenced through 40-50 lines at 5kHz only one selected line was transmitted. However, the mechanical system is hard to align and is limited in speed. This pulse-picking function has now been replaced with an acousto-optic modulator for the Pyrocam and the spectrometer has been replaced with an acousto-optically-tuned spectrometer. These rapid diagnostics will be the subject of a future paper.

#### 6. FUTURE WORK

As indicated in Table 1, our goals include increasing repetition rates to 100kHz or more and decreasing pulse lengths to

20ns or less, and possibly to produce mode-locked pulses as short as 2 ns. We have begun experiments to evaluate the CO<sub>2</sub> modules used in this system and other modules with smaller waveguides operating at higher gas pressures. We also plan to investigate the use of a phase shift between the two AO modulators of the tuner to change the effective cavity length. This would allow us to implement frequency stabilization of a rapidly-tuned laser. As well we plan to investigate the effect of a frequency shift between the two AOM's.

In the area of further development of AO tuning technology, the development of more compact devices and devices with better thermal characteristics should improve the technique, particularly for application to even higher tuning rates. Devices made of materials other than Ge might also result in significant improvements.

## 7. ACKNOWLEDGEMENTS

The authors would like to thank all the members of this LIDAR project for their assistance and helpful suggestions. In particular, thanks are due to Joe Tice, Mike Whitehead, Bernie Foy and other users of this system for their patience and input. Thanks also to Chuck Fite, Paul Johnson and Karla Atkins for their work in developing the control system. This research was fully supported by the U.S. Department of Energy under contract W-7405-ENG-36.

## 8. REFERENCES

1. S. Holly and S. Aiken, "Carbon Dioxide Probe Laser with Rapid Wavelength Switching", *Proc. SPIE* **122**, pp. 45-52, 1977.
2. A. Crocker, R.M. Jenkins, and M. Johnson, "A Frequency Agile, Sealed-Off CO<sub>2</sub> TEA Laser", *J. Phys. E* **18**, pp. 133-135, 1985.
3. S. Gotoff, et al, *Proc. SPIE* ??, pp. ???-???, 199?.
4. F.R. Faxvog and H. W. Mockler, "Rapidly Tunable CO<sub>2</sub> TEA Laser", *Appl. Opt.* **21**, pp. 3986-3987, 1982.
5. J.E. Eberhardt, J.G. Haub, and L.B. Whitbourn, "Carbon dioxide laser tuning through 110 lines in 3 ms for airborne remote sensing", *Appl. Opt.* **27**, pp. 879-884, 1988.
6. *Design and Fabrication of Acousto-Optic Devices*, A.P. Goutzoulis and D.R. Pape, eds., Marcel Dekker, Inc., New York, 1994.
7. W.R. Klein and B.D. Cook, "Unified Approach to Ultrasonic Light Diffraction", *IEEE Trans. Sonics and Ultrasonics*, **SU-13**, pp. 123-134, 1967.
8. R.V. Johnson, "Design of Acousto-Optic Modulators", *Design and Fabrication of Acousto-Optic Devices*, A.P. Goutzoulis and D.R. Pape, eds., pp. 123-193, Marcel Dekker, Inc., New York, 1994.
9. D.J. Taylor, S.E. Harris, S.T.K. Nieh and T.W. Hansch, "Electronic Tuning of a Dye Laser Using the Acousto-Optic Filter", *Appl. Phys. Lett.* **19**, pp. 269-271, 1971.
10. L.D. Hutcheson and R.S. Hughes, "Rapid Acousto-Optic Tuning of a Dye Laser", *Appl. Opt.* **13**, pp. 1395-1398, 1974.
11. K. Doughty and K. Cameron, "Electron Tuning of LEC Lasers", *Proc. SPIE* **1703**, pp. 136-142, 1992.

12. G.A. Coquin and K.W. Cheung, "Electronically Tunable External-Cavity Semiconductor Laser", *Electron. Lett.*, **24**, pp. 599-600, 1988.
13. L.J. Denes, M. Gottlieb, N.B. Singh, D.R. Suhre, H. Buhay, and J.J. Conroy, "Rapid Tuning Mechanism for CO<sub>2</sub> Lasers", *Proc. SPIE 894*, pp. 78-85, 1988.
14. W. Streifer and J.R. Whinnery, "Analysis of a Dye Laser Tuned by an Acousto-optic Filter", *Appl. Phys. Lett.* **17**, pp. 335-337, 1970.

Further author information -

D.C.T.(correspondence): Email: dcthomp@lanl.gov; Telephone: 505-667-5168; Fax: 505-665-4026

G.E.B.: Email: gbusch@lanl.gov; Telephone: 505-665-1941; Fax: 665-4267

C.J.H.: Email: c\_hewitt@lanl.gov; Telephone: 505-667-5817

D.K.R.: Email: dennisr@lanl.gov; Telephone: 505-665-0797

T.S.: Email: tsu@lanl.gov; Telephone: 505-667-8391

C.E.M.S.: Email: cems@lanl.gov

C.W.W.: Email: c\_wilson@lanl.gov; Telephone: 505-667-5817